Antiferromagnetic complexes with metal–metal bonds

XXV *. Synthesis, molecular structure and magnetic properties of the triangular cluster $Cp_2Cr_2(\mu\text{-}SCMe_3)(\mu_3\text{-}S)_2Ir(CO)(PPh_3)$ and the octanuclear cluster $Cp_2Cr_2(\mu_3\text{-}S)_2(\mu_4\text{-}S)Rh_2[Cp_2Cr_2(\mu\text{-}SCMe_3)(\mu_3\text{-}S)_2]_2$ with an unusual triangular heterometalloornament framework

A.A. Pasynskii *, I.L. Eremenko, V.R. Zalmanovitch, V.V. Kaverin, B. Orazsakhatov, S.E. Nefedov, O.G. Ellert, V.M. Novotortsev

N.S. Kurnakov Institute of General and Inorganic Chemistry of the Academy of Sciences of the USSR, 31 Leninsky Prosp., 117907 Moscow (USSR)

A.I. Yanovsky and Yu.T. Struchkov

A.N. Nesmeyanov Institute of Organoelement Compounds of the Academy of Sciences of the USSR, 28 Vavilov Street, 117813 Moscow (USSR)

(Received January 8th, 1991)

Abstract

The antiferromagnetic cluster $Cp_2Cr_2(\mu\text{-}SCMe_3)(\mu_3\text{-}S)_2Ir(CO)(PPh_3)$ (II) ($-2J = 324$ cm^{-1}) has been obtained by prolonged refluxing of $Cp_2Cr_2(\mu\text{-}SCMe_3)_2(\mu\text{-}S)$ (I) with equimolar $(Ph_3P)_2Ir(CO)Cl$ in toluene. According to X-ray structural analysis (space group $P2_1/n$, $a = 12.226(1)$, $b = 12.086(1)$, $c = 22.528(2)$ Å, $\beta = 98.975(8)°$, $V = 3288.1$ Å^3, $Z = 4$) II has a Cr_2Ir triangular metal core with loosened Ir–Cr bonds (3.229(2) and 3.034(1) Å) and an ordinary Cr–Cr bond (2.714(2) Å). The analogous reaction of I with $(Ph_3P)_2Rh(CO)Cl$ results in formation of a cluster $Cp_2Cr_2(\mu\text{-}SCMe_3)(\mu_3\text{-}S)_2Rh(CO)(PPh_3)$ (IV) ($-2J = 418$ cm^{-1}), which is presumably isostructural to the cluster II. Interaction of I with $[(C_2H_4)_2RhCl]_2$ (the Cr/Rh ratio of $2:1$) in benzene results in formation of an octanuclear antiferromagnetic cluster $Cp_2Cr_2(\mu_3\text{-}S)_2(\mu_4\text{-}S)Rh_2[Cp_2Cr_2(\mu\text{-}SCMe_3)(\mu_3\text{-}S)_2]_2$ (V) (μ_{eff} 1.59 (296 K)–1.29 (77 K) μ_B). According to X-ray structural data (space group $P\bar{1}$, $a = 10.470(6)$, $b = 14.253(7)$, $c = 18.340(1)$ Å, $\alpha = 81.09(1)$, $\beta = 86.28(1)$, $\gamma = 85.91(1)°$, $V = 2692.9$ Å^3, $Z = 2$) III has a central fragment Rh_2Cr_2 in the form of a butterfly with $RhCr_2$ wings (Rh–Cr 2.766(2)–2.754(2) Å, and the angle between $RhCr_2$ planes 129.8°) and short Cr–Cr bond distance (2.560(3) Å). One of the sulphur atoms is located between the wings (Rh–S$_{av}$ 2.369(4); Cr–S$_{av}$ 2.268(4) Å), while the other two sulphur atoms are located under the $RhCr_2$ wings of the butterfly (Rh–S$_{av}$ 2.253(4), Cr–S$_{av}$ 2.265(4) Å). Besides, each Rh atom is connected with the $Cp_2Cr_2(\mu\text{-}SCMe_3)(\mu_3\text{-}S)_2$ fragment (Cr–Cr 2.646(3) and 2.651(4) Å) by two Rh–Cr bonds (2.794(2)–2.826(2) Å) and two Rh–S bonds (2.323(4) Å).

---

* For Part XXIV see ref. 12.

Introduction

We have recently shown that the geometry of the metal triangular framework of the clusters $Cp_2Cr_2(\mu\text{-}SCMe_3)(\mu_3\text{-}S)_2ML_n$ depends to a considerable extent both on the electron state of the ML_n fragment and on the ligands surrounding the M atom [1]. For instance, if $ML_n = Co(CO)_2$ a stable triangular Cr_2Co framework (Cr–Cr 2.617, Cr–Co 2.592 Å) with tetrahedrally coordinated Co atom is formed in the cluster $Cp_2Cr_2(\mu\text{-}SCMe_3)(\mu_3\text{-}S)_2Co(CO)_2$ [2]. The situation changes drastically if $Co(CO)_2$ is replaced by $Rh(CO)_2$ or $Rh(\pi\text{-}C_8H_{12})$ [3]. In both cases the Rh^I atom has a typical planar-square coordination with a practically non-bonding Cr–Rh distance (3.0–3.1 Å) [3]. On the other hand, if the ligand surrounding the Rh atom differs greatly from square-planar as, e.g., in a spirane complex $Cp_2Cr_2(\mu\text{-}SCMe_3)(\mu_3\text{-}S)_2Rh(\mu_3\text{-}S)_2Fe_2(CO)_6$ (with the S_2Rh/RhS_2 angle of 130°), the single Rh–Cr bonds with the length of 2.720 and 2.724 Å may also be formed [4]. In order to clear up the situation we have synthesized a triangular cluster with a Cr_2Rh framework and nonequivalent substituents at the Rh atom. Besides, we have studied the behaviour of the corresponding iridium complex. We have also studied reactions of $Cp_2Cr_2(\mu\text{-}SCMe_3)_2(\mu\text{-}S)$ (I) with $[(C_2H_4)_2RhCl]_2$, containing two ethylene molecules which can readily be substituted.

Results and discussion

The prolonged refluxing of $Cp_2Cr_2(\mu\text{-}SCMe_3)_2(\mu\text{-}S)$ (I) with $(Ph_3P)_2M(CO)Cl$ (M = Rh, Ir) in toluene results in formation of the triangular clusters $Cp_2Cr_2(\mu\text{-}SCMe_3)(\mu_3\text{-}S)_2M(CO)(PPh_3)$ in the case of both metals.
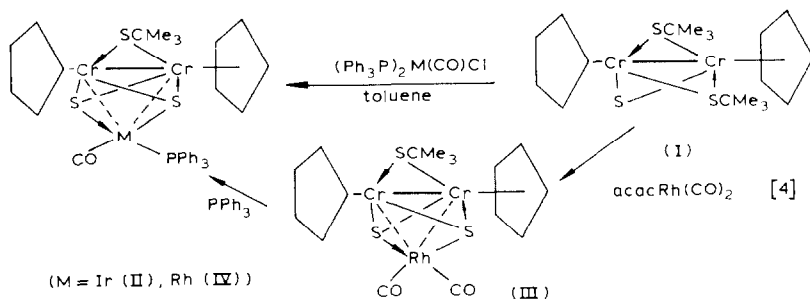
Cluster IV has been also obtained by the interaction of PPh_3 with the above mentioned cluster III.

In the IR-spectrum of II strong stretching bands of the terminal CO groups are registered at 1935 cm^{-1}. The cluster has antiferromagnetic properties and μ_{eff} decreases from 1.67 to 1.18 μ_B in the range of 276–77 K, which corresponds to the exchange parameter $-2J = 324$ cm^{-1}, calculated in accordance with the Heisenberg–Dirac–van Vleck model [5] for the two Cr^{III} ions with $S_1 = S_2 = 3/2$ (the Ir atom in this cluster has a 16-electron surrounding and is diamagnetic).

Cluster $Cp_2Cr_2(\mu\text{-}SCMe_3)(\mu_3\text{-}S)_2Rh(CO)(PPh_3)$ (IV) has been isolated in the form of large black-brown antiferromagnetic crystals (μ_{eff} decreases from 1.28 to 0.58 μ_B in the temperature range of 293–77 K, $-2J = 418$ cm^{-1}), and the strong band at 1940 cm^{-1} in the IR spectrum corresponds to stretching vibrations of the terminal CO-group.
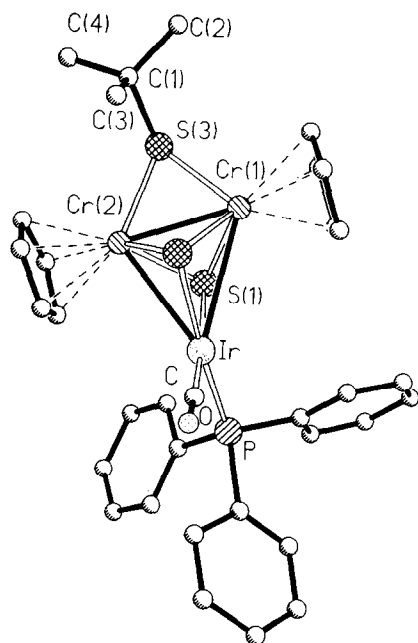
Fig. 1. The molecular structure of cluster $Cp_2Cr_2(\mu\text{-}SCMe_3)(\mu_3\text{-}S)_2Ir(CO)(PPh)$ (II).

According to the data of X-ray structural analysis (Fig. 1, Table 1) the geometry of the metal framework in II is analogous to that known for III. The Cr_2Ir framework has a single Cr–Cr bond (2.714(2) Å); however, there are two Cr–Ir bonds (3.229(2) and 3.034(1) Å). The Ir-atom has a planar-square coordination formed by two sulphur atoms (Ir–S 2.408(2) and 2.385(2) Å), and the carbon atom of the CO group (Ir–C 1.844(8) Å). Interestingly despite the difference between CO and PPh_3, the Ir–S bonds are practically equivalent (Table 1). It is also noteworthy

Table 1

Comparison of the geometrical characteristics of the triangular clusters $Cp_2Cr_2(\mu\text{-}SCMe_3)(\mu_3\text{-}S)_2ML_n$

	II, $ML_n = Ir(CO)(PPh_3)$	III, $ML_n = Rh(CO)_2$	IIIa, $ML_n = RhCOD$ [a]
Cr–Cr (Å)	2.714(2)	2.708(1)	2.686(2); 2.688(2)
M–Cr (Å)	3.229(2)	3.134(1)	3.064(1); 3.009(1)
	3.034(1)	3.010(1)	3.038(1); 3.019(1)
M–μ_3-S (Å)	2.408(2)	2.363(1)	2.359(1); 2.356(1)
	2.385(2)	2.381(1)	2.368(1); 2.353(1)
Cr–μ-SCMe_3 (Å)	2.364(2)	2.364(1)	2.362(2); 2.363(2)
	2.355(2)	2.348(1)	2.358(2); 2.369(2)
Cr–μ_3-S (Å)	2.302(2)–2.325(2)	2.314(1)–2.326(1)	2.297(2)–2.310(2)
μ_{eff} (MB)	1.67 (295 K)–1.13 (80 K)	0.78 (295 K)–0.58 (90 K)	1.17 (295 K)–0.89 (90 K)
$-2J$(Cr–Cr) (cm^{-1}) 324		592	568

[a] Unit cell contains two independent molecules.

that the geometry of the metal framework is only slightly influenced both by the substitution of Ir atom by Rh and of CO and PPh$_3$ ligands by π-cyclooctadiene.

However, it is noteworthy that the situation changes considerably if instead of [C$_8$H$_{12}$RhCl]$_2$ the isoelectronic [(C$_2$H$_4$)$_2$RhCl]$_2$ complex is used as the Rh-containing component, as the latter contains ethylene molecules which can be readily substituted by other donor ligands. Interaction of I with [(C$_2$H$_4$)$_2$RhCl]$_2$ turned out to result in formation of an octanuclear cluster Cp$_2$Cr$_2$(μ_3-S)$_2$(μ_4-S)Rh$_2$[Cp$_2$Cr$_2$(μ-SCMe$_3$)(μ_3-S)$_2$]$_2$ (V) at room temperature:

(I)   (Ⅴ)
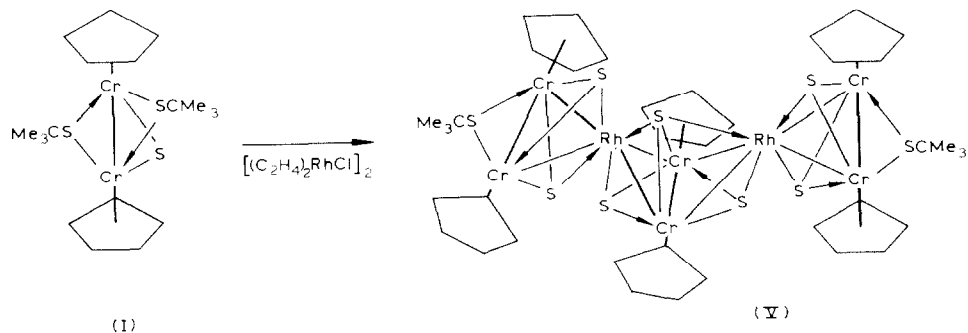
V has been isolated in the form of black prismatic antiferromagnetic crystals (μ_{eff} decreases from 1.59 to 1.29 μ_B in the temperature range of 296–77 K). The IR spectrum of the cluster contains bands of Cp-rings (795, 1065, 3040 cm^{-1}) and tert-butyl groups (1150, 2845, 2950 cm^{-1}). The structure of V has been solved by means of X-ray structural analysis (Fig. 2, Table 2). The cluster contains a central butterfly core Cr$_2$Rh$_2$ in which short Cr–Cr (2.560(3) Å) and Cr–Rh (2.754(2)–2.766(2) Å) bonds are supplemented by a μ_4-sulphide bridge located between the RhCr$_2$ wings and two μ_3-sulphide bridges located below the wings of the butterfly (the Cr$_2$Rh/RhCr angle is 129.8°). As a whole the geometry of the butterfly core resembles the earlier studied cluster, CpCo(Cp$_2$Cr$_2$S$_3$)CoCp (Cr–Cr 2.585, Co–Cr 2.660 Å, with the angle between the Cr$_2$Co/CoCr$_2$ planes 128.0°) [6]. Besides, in V
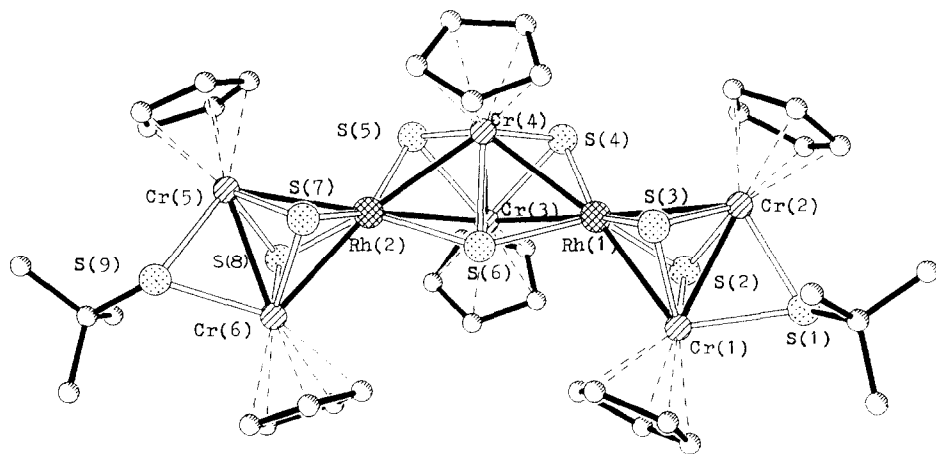

Fig. 2. The molecular structure of cluster Cp$_2$Cr$_2$(μ_3-S)$_2$(μ_4-S)Rh$_2$[Cp$_2$Cr$_2$(μ-SCMe$_3$)(μ_3-S)$_2$]$_2$ (V).

Table 2

The main geometric data of cluster $Cp_2Cr_2(\mu_3\text{-S})_2(\mu_4\text{-S})Rh_2[Cp_2Cr_2(\mu\text{-SCMe}_3)(\mu_3\text{-S})_2]_2\cdot2C_6H_6$ (V)

Bond lengths (Å)		Bond angles (°)	
Rh(1)–Cr(1)	2.794(3)	Cr(1)Rh(1)Cr(2)	56.48(7)
Rh(1)–Cr(2)	2.797(2)	Cr(3)Rh(1)Cr(4)	55.34(7)
Rh(1)–Cr(3)	2.760(3)	Cr(3)Rh(2)Cr(4)	55.10(7)
Rh(1)–Cr(4)	2.754(3)	Cr(5)Rh(2)Cr(6)	56.35(7)
Rh(2)–Cr(3)	2.766(2)	Rh(1)Cr(1)Cr(2)	61.83(7)
Rh(2)–Cr(4)	2.759(2)	Rh(1)Cr(2)Cr(1)	61.69(7)
Rh(2)–Cr(5)	2.788(3)	Rh(1)Cr(3)Rh(2)	106.41(8)
Rh(2)–Cr(6)	2.826(3)	Rh(1)Cr(3)Cr(4)	62.21(8)
Cr(1)–Cr(2)	2.646(3)	Rh(2)Cr(3)Cr(4)	62.12(8)
Cr(3)–Cr(4)	2.560(3)	Rh(1)Cr(4)Rh(2)	107.04(8)
Cr(5)–Cr(6)	2.651(4)	Rh(1)Cr(4)Cr(3)	62.45(8)
Rh–μ_4-S	2.370(4)	Rh(2)Cr(5)Cr(6)	62.54(8)
	2.367(4)	Rh(2)Cr(4)Cr(3)	62.78(8)
		Rh(2)Cr(6)Cr(5)	61.11(8)
Rh–μ_3-S	2.252(4)–2.334(4)	Rh(2)μ_4-SRh(1)	138.8(2)
Cr–μ_4-S	2.260(4)	Cr(3)μ_4-SCr(4)	68.7(1)
	2.276(4)	$Cr_2Rh(1)/Cr_2Rh(1)$	119.3
Cr–μ_3-S	2.265(4)–2.295(4)	$Cr_2Rh(2)/Cr_2Rh(2)$	121.8
Cr–μ-SCMe$_3$	2.343(5)–2.359(4)	$Cr_2Rh(1)/Cr_2Rh(2)$	129.8

each rhodium atom is strongly connected with the dichromic $Cp_2Cr_2(\mu\text{-SCMe}_3)(\mu\text{-S})_2$ fragment (Cr–Cr 2.646(3) and 2.651(3) Å) via two sulphide bridges and direct Cr–Rh bonds (2.788(3)–2.826(3) Å). As a result the cluster has two spirane fragments Cr_2RhCr_2 (the angles Cr(1)Cr(2)Rh(1)/Rh(1)Cr(3)Cr(4) and Cr(5)Cr(6) Rh(2)/Rh(2)Cr(3)Cr(4) are 119.34 and 121.8° respectively) with the common central axis Cr–Cr. In contrast to the above mentioned clusters which have a Cr_2Rh framework with the square-planar coordination of Rh[I] atoms, V contains Rh[II] ions with ligand coordination close to the tetrahedral (Rh(1)S(2)S(3)/Rh(1)S(4)S(6) 119.7°, Rh(2)S(5)S(6)/Rh(2)S(7)S(8) 122.0°). The dihedral angles S_2Rh/RhS_2 in two spirane fragments differ only by 2.3° with the values (130°) close to that observed in the spirane cluster $Cp_2Cr_2(\mu\text{-SCMe}_3)(\mu_3\text{-S})_2Rh(\mu_3\text{-S})_2Fe_2(CO)_6$ [4].

It should be emphasized that cluster V is a first example of the triangular heterometalloornament $Cr_2RhCr_2RhCr_2$ which differs from the cluster with the $Fe_2CoCr_2CoFe_2$ core which we described previously [7]. It consists, indeed, of a succession of closed triangles. Besides, as cluster V contains functional $Cr_2(\mu\text{-SCMe}_3)$ groups it is presumably capable of further elongation of the framework chain of triangles. For instance it is noteworthy that besides crystals V an amorphous substance has also been isolated from the reaction mixture whose IR spectrum practically coincides with that of V. The amorphous substance probably consists of the homologues of the cluster V with higher molecular weight.

Experimental

All operations connected with synthesis of initial and final clusters were carried out in a flow of pure argon in absolute solvents. IR-spectra were measured with a

Table 3

Atomic coordinates (for Ir, Cr, S and $P \times 10^5$, for O and $C \times 10^4$) for the cluster $Cp_2Cr_2(SCMe_3)(\mu_3\text{-}S)_2Ir(CO)(PPh_3)$ (II)

Atom	x	y	z
Ir	42631(3)	11084(3)	30833(1)
Cr(1)	40189(11)	13562(11)	16415(5)
Cr(2)	47108(11)	−5983(11)	21630(5)
S(1)	55415(16)	11153(20)	23712(8)
S(2)	30698(16)	3096(18)	22557(9)
S(3)	46307(16)	−1832(18)	11355(9)
P	55074(16)	19529(17)	37911(9)
O	2421(5)	864(6)	3793(3)
C	3153(7)	981(7)	3547(3)
C(1)	3554(7)	−989(8)	617(4)
C(2)	3236(8)	−290(9)	41(4)
C(3)	2526(7)	−1195(9)	918(4)
C(4)	4124(9)	−2077(9)	478(5)
C(5)	4470(9)	2733(8)	1057(5)
C(6)	3403(10)	2339(9)	822(4)
C(7)	2662(9)	2517(9)	1233(5)
C(8)	3288(8)	3066(8)	1737(4)
C(9)	4397(9)	3193(8)	1633(5)
C(10)	4723(9)	−1760(9)	2933(5)
C(11)	4326(10)	−2314(9)	2415(6)
C(12)	5159(10)	−2364(9)	2084(5)
C(13)	6083(9)	−1806(10)	2415(6)
C(14)	5756(8)	−1438(8)	2945(5)
C(15)	6833(6)	1231(7)	4031(3)
C(16)	7487(7)	971(8)	3597(4)
C(17)	8481(7) −	396(8)	3759(5)
C(18)	8803(7)	63(8)	4375(4)
C(19)	8156(7)	336(8)	4795(4)
C(20)	7167(7)	932(7)	4641(4)
C(21)	5901(6)	3301(6)	3530(3)
C(22)	6987(6)	3725(7)	3663(3)
C(23)	7197(7)	4785(8)	3435(4)
C(24)	6359(8)	5422(7)	3125(4)
C(25)	5293(8)	5003(7)	3016(4)
C(26)	5053(7)	3947(7)	3219(4)
C(27)	5087(6)	2300(6)	4523(3)
C(28)	4518(7)	1500(7)	4797(3)
C(29)	4198(8)	1769(8)	5363(4)
C(30)	4438(7)	2800(7)	5627(4)
C(31)	5032(7)	3555(7)	5351(4)
C(32)	5361(7)	3323(7)	4785(3)

Specord 75IR instrument in KBr pellets. Magnetic susceptibility was measured by the Faraday method using the technique developed in the Institute of General and Inorganic Chemistry of the Academy of Sciences of the USSR [8]. Calculations of the exchange parameters were carried out according to the Heisenberg–Dirac–van Vleck model using the SM-4 computer. Experimental data for X-ray structural study have been obtained with automatic diffractometers Hilger & Watts (II) and Syntex

Table 4

Atomic coordinates (for Rh and $Cr \times 10^5$, for S and $C \times 10^4$) for the cluster $Cp_2Cr_2(\mu_3\text{-}S)_2(\mu_4\text{-}S)Rh_2[Cp_2Cr_2(\mu\text{-}SCMe_3)(\mu_3\text{-}S)_2]_2 \cdot 2C_6H_6$ (V)

Atom	x	y	z
Rh(1)	29034(12)	22694(8)	41139(6)
Rh(2)	47314(12)	23699(7)	18566(6)
Cr(1)	3062(24)	20127(15)	44774(12)
Cr(2)	16644(24)	26499(15)	54439(12)
Cr(3)	46086(24)	12867(15)	32513(12)
Cr(4)	48093(24)	30803(15)	31686(12)
Cr(5)	57579(25)	29603(15)	4318(12)
Cr(6)	34880(26)	22191(16)	5611(12)
S(1)	−435(4)	2173(2)	5697(2)
S(2)	2010(4)	1208(2)	5059(2)
S(3)	1257(4)	3421(2)	4282(2)
S(4)	5040(4)	2030(2)	4210(2)
S(5)	6282(4)	2084(3)	2672(2)
S(6)	3099(4)	2423(2)	2807(2)
S(7)	3924(4)	3577(2)	982(2)
S(8)	5373(4)	1435(2)	947(2)
S(9)	4406(4)	2997(3)	−553(2)
C(1)	−1741(15)	3124(10)	5797(8)
C(2)	−1616(15)	3444(11)	6545(8)
C(3)	−2983(17)	2661(11)	5744(11)
C(4)	−1604(18)	3992(10)	5204(8)
C(5)	4956(18)	2223(11)	−1275(8)
C(6)	3746(20)	2007(14)	−1649(9)
C(7)	5908(22)	2852(13)	−1817(9)
C(8)	5688(19)	1289(10)	−945(9)
Cp(11)	373(15)	1351(9)	3421(7)
Cp(12)	−311(17)	733(11)	4051(7)
Cp(13)	−1380(15)	1271(12)	4287(8)
Cp(14)	−1464(15)	2179(8)	3918(8)
Cp(15)	−417(17)	2225(11)	3354(8)
Cp(21)	2637(15)	2306(10)	6496(8)
Cp(22)	1722(18)	3052(10)	6551(8)
Cp(23)	2070(16)	3831(10)	6029(8)
Cp(24)	3220(17)	3551(11)	5646(8)
Cp(25)	3584(15)	2610(11)	5925(8)
Cp(31)	4894(25)	13(11)	2708(12)
Cp(32)	2651(20)	63(10)	2935(12)
Cp(33)	3647(21)	−17(10)	3733(10)
Cp(34)	4962(27)	−91(10)	3881(11)
Cp(35)	5700(23)	−75(11)	3233(17)
Cp(41)	4015(9)	4540(9)	2822(8)
Cp(42)	5289(17)	4435(9)	2471(8)
Cp(43)	6184(16)	4216(10)	3035(9)
Cp(44)	5499(18)	4221(10)	3734(9)
Cp(45)	4171(16)	4402(9)	3608(8)
Cp(51)	7313(15)	3542(10)	958(8)
Cp(52)	7880(16)	2786(10)	634(9)
Cp(53)	7750(18)	2984(12)	−139(12)

Table 4 (continued)

Atom	x	y	z
Cp(54)	7037(19)	3936(12)	−258(9)
Cp(55)	6824(15)	4256(10)	419(9)
Cp(61)	1315(16)	2423(12)	578(8)
Cp(62)	1701(16)	1800(15)	1228(8)
Cp(63)	2351(20)	992(13)	1031(11)
Cp(64)	2382(17)	1077(12)	276(10)
Cp(65)	1757(19)	1977(13)	11(10)
$C_b(1)$	1363(17)	4565(11)	7890(9)
$C_b(2)$	480(19)	5165(13)	7493(11)
$C_b(3)$	−554(20)	5475(13)	7832(13)
$C_b(4)$	−782(20)	5280(11)	8607(14)
$C_b(5)$	129(22)	4654(13)	9030(10)
$C_b(6)$	1233(18)	4303(11)	8675(10)
$C_b(7)$	984(22)	6(15)	8917(10)
$C_b(8)$	1398(18)	−279(11)	8264(10)
$C_b(9)$	868(21)	122(12) −	7611(9)
$C_b(10)$	−127(22)	806(15)	7634(11)
$C_b(11)$	−545(19)	1116(13)	8311(12)
$C_b(12)$	0(20)	693(13)	8934(10)

Table 5

Crystal data for the clusters $Cp_2Cr_2(\mu\text{-SCMe}_3)(\mu_3\text{-S})_2Ir(Co)(PPh_3)$ (II) and $Cp_2Cr_2(\mu_3\text{-S})_2(\mu_4\text{-S})Rh_2[Cp_2Cr_2(\mu\text{-SCMe}_3)(\mu_3\text{-S})_2]_2\cdot2C_6H_6$ (V)

	II	V
Crystal system	Monoclinic	Triclinic
Space group	$P2_1/n$	$P\bar{1}$
a (Å)	12.226(1)	10.470(6)
b (Å)	12.086(1)	14.253(7)
c (Å)	22.528(2)	18.340(1)
α (°)	90	81.09(1)
β (°)	98.975(8)	86.28(1)
γ (°)	90	85.91(1)
V (Å^3)	3288.1	2692.9
Z	4	2
Number of reflections measured	5128	7039
Number of reflections with $I > 4\sigma$	3930	5992
R_1	0.034	0.064
R_w	0.039	0.069

$P2_1$ (V) at 20°C. Calculations were carried out on an Eclipse S/200 computer (EXTL programme package) (Tables 3–5).

Syntheses of $Cp_2Cr_2(\mu\text{-SCMe}_3)_2S$, $Ir(PPh_3)_2(CO)Cl$, and $[Rh(C_2H_4)_2Cl]_2$ have been performed in accordance with the techniques described in ref 9, 10, and 11, respectively *.

---

* The authors express their gratitude to Dr. Yu.S. Varshavsky for the samples of $Ir(PPh_3)_2(CO)Cl$ and $[Rh(C_2H_4)_2Cl]_2$.

Cp₂Cr₂(μ-SCMe₃)(μ₃-S)₂Ir(CO)(PPh₃) (II)

$Cp_2Cr_2(\mu\text{-}SCMe_3)(\mu_3\text{-}S)_2Ir(CO)(PPh_3)$ (II)

10 ml of the toluene solution containing 0.28 g (0.64 mM) of $Cp_2Cr_2(\mu\text{-}SCMe_3)_2S$ was added to the yellow solution containing 0.5 g (0.64 mM) of $Ir(CO)(Cl)(PPh_3)_2$ in 50 ml of toluene under refluxing. The blue-violet mixture was refluxed for 10 hours. The solution thus formed was evaporated to dryness at 60°C/10 torr and extracted by 30 ml of acetone. The brown extract was concentrated at 20°C/10 torr to the volume of 10 ml. Within 48 h at room temperature black-brown crystals of complex II suitable for X-ray structural investigation were precipitated: Yield 0.26 g (41%).

IR spectrum (ν, cm^{-1}): 495s, 515vs, 570w, 685vs, 740s, 785s, 800s, 985w, 1000w, 1085s, 1145m, 1420m, 1480m, 1935vs.

$Cp_2Cr_2(\mu_3\text{-}S)_2(\mu_4\text{-}S)Rh_2[Cp_2Cr_2(\mu\text{-}SCMe_3)(\mu_3\text{-}S)_2]_2 \cdot 2C_6H_6$ (V)

25 ml of the orange benzene solution containing 0.1 g (0.25 mM) of $[Rh(C_2H_4)_2Cl]_2$ was added dropwise to 10 ml of the violet benzene solution of 0.23 g (0.5 mM) of $Cp_2Cr_2(\mu\text{-}SCMe_3)_2S$. The brown solution formed was covered with a layer of heptane. With three days at room temperature black prisms precipitated on the benzene–heptane border; they were isolated from the solution by decantation, washed in heptane and dried in vacuo: Yield 0.18 g (14%).

IR spectrum (ν, cm^{-1}): 620vw, 795vs, 1015m, 1065w, 1150vs, 1350m, 1435s, 1620m, 2845w, 2880w, 2910m, 2950w.

References

1 A.A. Pasynskii and I.L. Eremenko, Sov. Sci. Rev., 10 (1987) 443.
2 A.A. Pasynskii, I.L. Eremenko, B. Orazsakhatov, O.G. Ellert, V.T. Kalinnikov, G.G. Aleksandrov and Yu.T. Struchkov, J. Organomet. Chem., 214 (1981) 351.
3 A.A. Pasynskii, I.L. Eremenko, V.R. Zalmanovitch, V.V. Kaverin, B. Orazsakhatov, V.M. Novotortsev, O.G. Ellert, A.I. Yanovsky and Yu.T. Struchkov, J. Organomet. Chem., 356 (1988) 57.
4 I.L. Eremenko, A.A. Pasynskii, A.S. Katugin, V.R. Zalmanovitch, B. Orazsakhatov, S.A. Sleptsova, A.I. Nechaev, V.V. Kaverin, O.G. Ellert, V.M. Novotortsev, A.I. Yanovsky, V.E. Shklover and Yu.T. Struchkov, J. Organomet. Chem., 365 (1989) 325.
5 J.H. van Vleck, The Theory of Electronic and Magnetic Susceptibilities, Oxford Univ. Press, London, 1932.
6 I.L. Eremenko, A.A. Pasynskii, A.S. Katugin, B. Orazsakhatov, V.L. Shirokii, V.E. Shklover and Yu.T. Struchkov, J. Organomet. Chem., 345 (1988) 177.
7 A.S. Katugin, A.A. Pasynskii, I.L. Eremenko, B. Orazsakhatov, A.S. Aliev, Yu.T. Struchkov and A.I. Yanovsky, J. Organomet. Chem., 382 (1990) 423.
8 V.M. Novotortsev, Ph.D. Thesis, Moscow, 1974.
9 A.A. Pasynskii, I.L. Eremenko, Yu.V. Rakitin, V.M. Novotortsev, V.T. Kalinnikov, G.G. Aleksandrov and Yu.T. Struchkov, J. Organomet. Chem., 165 (1979) 57.
10 J.P. Collman and J.W. Kang, J. Am. Chem. Soc., 89 (1967) 844.
11 E.L. Smutni, H. Chung, K.C. Dewhirst, W. Kein, T.M. Shryne and H.E. Thyret, Am. Chem. Soc., Div. Pet. Chem., Prepr., 14 (1969) B100.
12 I.L. Eremenko, A.A. Pasynskii, E.A. Vas'utinskaya, A.S. Katugin, S.E. Nefedov, O.G. Ellert, V.M. Novotortsev, A.F. Shestakov, A.I. Yanovsky and Yu.T. Struchkov, J. Organomet. Chem., 411 (1991) 193.